Lab on a Chip

PAPER

View Article Online
View Journal

Cite this: DOI: 10.1039/d6lc00118a

An automated modular microfluidic platform for end-to-end mRNA synthesis and purification

Vikas Sharma, † Amirreza Mottafegh,† Jeong-Un Joo† and Dong-Pyo Kim *

Manual, batchwise downstream operations remain a major bottleneck in translating microfluidic mRNA synthesis into practical production workflows. Building on an oscillatory microfluidic IVT module (Os(IVT)) previously established for intensified transcription, here we introduce an end-to-end, automated, modular lab-on-a-chip platform that integrates transcription with inline nucleic-acid processing and purification. The workflow couples Os(IVT) to a newly developed microfluidic digestion/clarification (μFD) unit, where DNase I immobilized on a biocatalytic membrane performs rapid template removal while a micro-tangential flow filtration (μ-TFF) step enables simultaneous buffer exchange/clarification without sacrificing full-length mRNA recovery. The processed stream is then routed to an automated multimodal chromatography (MMC) module governed by real-time pH and conductivity feedback to reproducibly gate binding, washing, and elution. Using firefly luciferase mRNA as a model, the fully integrated Os(IVT)–μFD–MMC workflow completed synthesis-to-purification in 2 h, delivered 1275 ± 1.7 μg mRNA per run *vs.* 641 ± 0.6 μg for the fully batch benchmark (~2.0×), with ~93.3% MMC recovery and an 83.3% reduction in dsRNA impurities relative to the batch workflow. This work advances oscillatory microfluidic IVT from a standalone intensified reactor to a closed-loop, end-to-end microfluidic manufacturing platform, enabling rapid, reproducible production of high-quality mRNA with substantially reduced manual handling.

Received 9th February 2026,
Accepted 4th April 2026

DOI: 10.1039/d6lc00118a

rsc.li/loc

1. Introduction

The emergence of mRNA modality has revolutionized modern medicine, enabling major advances in vaccine development and opening new opportunities in cancer immunotherapy and other therapeutic areas. mRNA has already demonstrated clinical success through approved vaccines, particularly for infectious diseases, yet its broader therapeutic application beyond vaccination is still largely at the investigational stage. The rapid success of mRNA-based COVID-19 vaccines has nevertheless highlighted the urgent need for efficient and cost-effective platforms to meet the growing demand for RNA-based biologics.[1] However, current mRNA manufacturing processes face persistent challenges due to inefficiencies in IVT and downstream processing. Traditional batch-IVT (B(IVT)) reactions are prone to inefficient mixing, poor heat dissipation, and uneven reagent distribution, which destabilize RNA polymerase and reduce mRNA yield.[2,3] Pyrophosphate accumulation further inhibits enzyme activity by chelating magnesium ions, even in the presence of pyrophosphatase.[4] Downstream processing is also a major cost driver, requiring removal of unincorporated nucleotides, residual DNA templates, enzymes, abortive transcripts, uncapped mRNA and immunogenic dsRNA contaminants. These steps are typically complex, multi-stage, and resource-intensive, often resulting in product loss and compromised mRNA integrity due to prolonged processing times.[5]

To overcome these limitations, flow-based automated and integrated platforms offer a promising alternative to manually operated, discrete unit operations.[2,6] Conventional workflows involve sequential steps including IVT, template digestion, desalting, purification, and concentration performed in separate systems, increasing time, handling, and contamination risk.[7] Integration and automation in biomanufacturing have shown clear benefits in productivity, facility utilization, and process consistency, and there is growing momentum to apply similar principles to mRNA production.[2,8–13] In particular, an automated flow-based platform can enable tighter control of residence time, mixing, and physicochemical conditions, while reducing operator dependence and supporting more reproducible product quality.[2,11]

Microfluidic systems are well-suited to implement such integrated workflows. Their high surface-to-volume ratios and precise flow control enhance mixing, heat transfer, and reaction uniformity, and they naturally lend themselves to modular unit-operation design and automation.[14] While microfluidics is widely used in chemical synthesis, diagnostics, and

Center for Intelligent Microprocess of Pharmaceutical Synthesis, Department of Chemical Engineering, Pohang University of Science and Technology (POSTECH), Pohang 37673, Republic of Korea. E-mail: dpkim@postech.ac.kr
† These authors contributed equally to this work.

nanoparticle production, microfluidic approaches for IVT-based mRNA synthesis and end-to-end processing remain comparatively underexplored.[15–18] A preliminary study by Choi *et al.*[3] demonstrated microfluidic IVT using micromixers, but broader adoption will require integrated, manufacturing-relevant workflows that couple intensified synthesis to streamlined downstream processing and quality control. In contrast, controlled microfluidic flow enables high precision, flexibility, and reproducibility, while the use of suitable device materials and surface modifications can reduce non-specific adsorption and fouling in polymer-based microfluidic systems.[19–21]

A major bottleneck for end-to-end integration is the transition from transcription to downstream cleanup. Biocatalytic membranes, enzyme-immobilized supports, offer an attractive route to inline bioprocessing due to catalytic efficiency, reusability, and compatibility with continuous operation.[22,23] In the context of mRNA, DNase digestion is essential for removing the residual DNA template, yet batch digestion typically adds hold time and introduces enzyme carryover risks. Immobilizing DNase I on polyethersulfone (PES) membranes enables rapid, selective template degradation in a membrane format that can be coupled directly to filtration-based clarification and buffer exchange, thereby compressing time and unit operations.[24] In parallel, automated chromatographic purification can further reduce downstream complexity. Multimodal chromatography (MMC), which combines electrostatic, hydrophobic, and hydrogen-bonding interactions, can provide high-resolution purification in fewer steps and has been explored for mRNA and other biomolecules.[2,7,9] Despite these advances, an automated, microfluidic, end-to-end mRNA workflow that integrates intensified IVT with inline template removal/clarification and sensor-guided chromatographic capture and polishing has not yet been demonstrated.

In this work, we present a centrally orchestrated computer-controlled microfluidic platform that consolidates key stages of mRNA production and purification into an automated, modular workflow (Fig. 1a). Building on our previously reported oscillatory IVT (Os(IVT)) unit operation,[25] we focus here on the

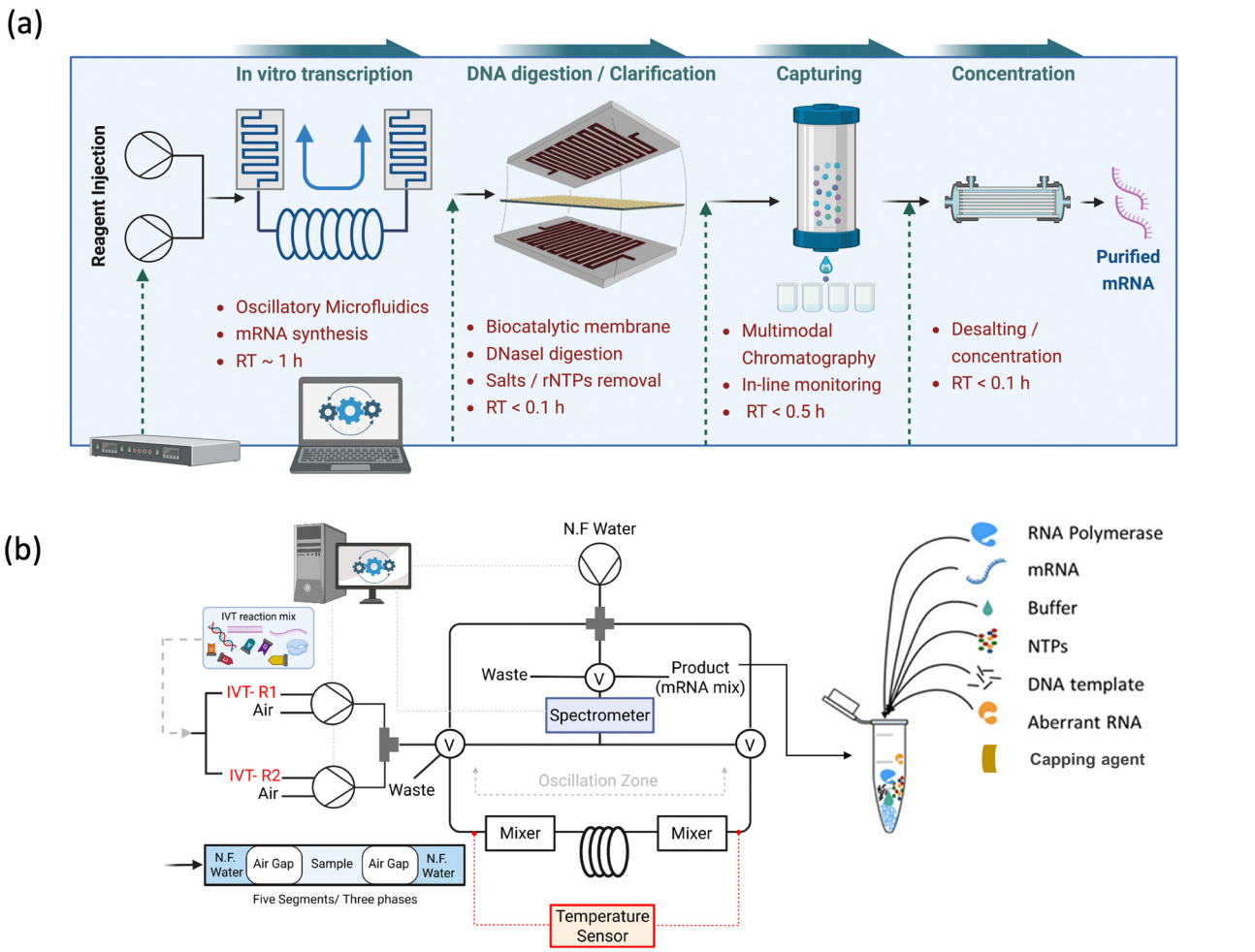

Fig. 1 Automated integrated microfluidic platform for quasi-continuous mRNA synthesis and purification. (a) End-to-end workflow comprising invitro transcription *via* Os(IVT), digestion/clarification using the μFD module, capturing step *via* multimodal chromatography (MMC), and concentration using hollow-fiber tangential flow filtration (HF-TFF); (b) schematic of unit operation A (Os(IVT)).

new end-to-end integration and downstream innovations. Specifically, we introduce a microfluidic digestion/clarification module (μFD) incorporating a DNase I-immobilized biocatalytic membrane coupled with tangential flow filtration (TFF) to enable one-step template digestion and removal of residual IVT components while preserving full-length mRNA. Downstream, the process is interfaced with an MMC monolith column (PrimaS, Sartorius AG) for capture and purification, equipped with integrated real-time pH and conductivity sensing to enable computer-regulated control of binding, washing and elution. The workflow concludes with desalting and concentration to produce high-quality mRNA. These modules are integrated into a unified platform denoted [Os(IVT)–μFD–MMC], enabling an automated synthesis-to-purification process that enhances mRNA yield, boosts protein expression, minimizes dsRNA contamination, and improves overall recovery and productivity. With a processing time of 2 h and an output of ~1200 μg mRNA per run, the platform demonstrates bench-scale, research- to preclinical-scale mRNA production with rapid and reproducible performance, providing a practical route toward modular, quasi-continuous manufacturing for both outbreak response and personalized therapeutic applications.

2. Results & discussion

2.1 Developing an automated and integrated microfluidic platform

The integrated platform comprises four automated unit operations arranged in sequence: Os(IVT) for mRNA synthesis, a microfluidic digestion/clarification module (μFD) for DNase I-mediated template removal and tangential-flow filtration, an automated multimodal chromatography (MMC) module with in-line pH and conductivity monitoring, and a hollow-fiber tangential flow filtration (HF-TFF) module for desalting and concentration. As shown in Fig. 1a, this modular arrangement enables automated transfer between synthesis and downstream processing and provides the framework for the module-by-module evaluation presented below.

2.2 Flow IVT by oscillatory microfluidics: unit operation A

The automated Os(IVT) bioreactor, previously reported as a standalone unit,[24] was operated here as unit operation A of the integrated platform. In a typical run, two IVT feed solutions were introduced by computer-controlled simultaneous co-injection (75 μL each, 1 : 1 ratio) to generate a 150 μL reaction segment. One feed contained the linearized FLuc DNA template, nucleotide triphosphates (NTPs), and cap analog, while the other contained T7 RNA polymerase and buffer. The reaction segment was assembled into a five-segment plug using nuclease-free water and air spacers (Fig. 1b and S1), confined within a defined oscillation zone, and repeatedly shuttled bidirectionally through PTFE serpentine micromixers (5 cm length, 500 μm cross-section) positioned at both ends of the capillary reactor (3.8 m) to promote rapid homogenization. An in-line spectrometer monitored fluid interfaces and triggered valve switching for flow reversal, thereby maintaining plug position within the programmed reaction zone and enabling automated routing of the crude IVT stream after completion of the residence time.

Under optimized operating conditions, the Os(IVT) bioreactor was run with micromixers at 1 mL min^{-1} and a capillary flow rate of 100 μL min^{-1}, providing a residence time of 60 min. The IVT reaction mixture contained 5 U μL^{-1} T7 RNA polymerase, 20 mM Mg^{2+}, and a cap analog-to-NTP molar ratio of 4 : 5, with the incubation temperature maintained at 37 °C. Under these conditions, the Os(IVT) process yielded 3310 ng μL^{-1} of FLuc mRNA in 1 h, representing a 346% increase compared to the 1 h batch process (955 ng μL^{-1}). In the previously reported standalone evaluation, Os(IVT)-derived mRNA showed 151% higher protein expression and 65% lower dsRNA than the 4 h batch benchmark under the same downstream assay conditions, indicating improved translation competence of the produced mRNA, rather than serving as a direct measure of IVT productivity.

Optimization of the cap analog-to-NTP ratio showed that protein expression could be further improved at a lower cap analog condition than that used in batch IVT, while also reducing reagent consumption.[24] These results underscore the efficiency of the Os(IVT) bioreactor as a core module for high-yield, high-quality mRNA synthesis within the integrated [Os(IVT)–μFD–MMC] manufacturing platform.

In our previously reported work,[25] multiple batch and microfluidic strategies for mRNA synthesis were systematically evaluated, with the microfluidic-based oscillatory module demonstrating the highest efficiency and reproducibility among all approaches. Mechanistically, Os(IVT) benefits from oscillatory flow reversal through serpentine micromixers, which repeatedly renews the boundary layer and minimizes concentration micro-heterogeneity within the reaction zone. This reduces local substrate depletion and improves effective enzyme–substrate contact over the programmed residence time, supporting higher mRNA accumulation and improved translational output. These effects are consistent with our previously reported Os(IVT) study, in which oscillatory micromixing and controlled residence time were identified as key contributors to improved yield and protein expression relative to batch operation. In that study, however, DNA template digestion was performed using a DNase I-catalyzed batch reaction, and purification was achieved *via* lithium chloride (LiCl) precipitation, both of which are time-intensive, less efficient, and incompatible for integrated continuous workflow. To overcome these limitations, the Os(IVT) process was incorporated into the present integrated platform as the Os(IVT) module (unit operation A), establishing the basis for continuous or quasi-continuous manufacturing of RNA therapeutics. This was complemented by the development of a novel biocatalytic membrane-assisted μFD module, followed by an automated MMC module, as described below, to streamline the integrated workflow for mRNA manufacturing.

2.3 Development of a microfluidic digestion (μFD) module

The crude mRNA obtained from the IVT reaction contains the target mRNA along with various impurities, including the residual DNA template, T7 RNA polymerase, unincorporated NTPs, aberrant or truncated mRNA species, and other reaction byproducts. To ensure efficient downstream purification, it is essential to remove the DNA template *via* DNase I digestion, followed by a filtration step to eliminate smaller impurities such as nucleotides. In conventional workflows, DNase I is added directly to the crude IVT mixture and incubated for approximately 30 min at 37 °C, after which TFF or direct chromatographic purification is performed. However, this approach prolongs processing time, which increases the risk of enzyme carryover, low mRNA recovery and compromised mRNA purity.[7]

To streamline downstream processing, we replaced the conventional batch-mode DNase I digestion followed by TFF with a single-step μFD module. This integrated unit combines DNA template degradation, using DNase I immobilized on a PES biocatalytic membrane, with a continuous microfluidic TFF (μ-TFF) unit, enabling simultaneous digestion and pre-removal of residual DNA fragments in a continuous-flow format. In this module, the retentate refers to the mRNA-containing retained fraction, while the permeate denotes the stream passing through the membrane that contains digested DNA fragments, unbound NTPs, and other small-molecule impurities. We selected a 30 nm pore PES membrane for its chemical stability, hydrophilicity, and facile surface chemistry.[26,27] In a study, α-amylase was covalently immobilized onto a polydopamine (Pdop)-functionalized PES membrane, which effectively preserved the activity of α-amylase enzyme and exhibited superior stability and strong antifouling properties.[24,26] The permeability test revealed that a membrane pore size of 30 nm is optimal for effective mRNA retention, whereas larger pore sizes result in undesired mRNA permeation through the membrane (Fig. S3(a)). Accordingly, a PES-Pdop-DNase I biocatalytic membrane was fabricated and embedded into a μ-TFF unit.

The preparation process is illustrated in Fig. S2(b) and detailed in section 3.3. The membrane surfaces were characterized by measuring the water contact angle, surface modification using X-ray Photoelectron Spectroscopy (XPS), and DNase I enzyme activity by performing the DNase I activity assay. The hydrophilic thin coated Pdop layer was confirmed by a drop in water contact angle from 68° to 26°, to introduce amine/catechol groups for enzyme attachment, to reduce non-specific adsorption of nucleic acids and enzymes (Fig. S3(b)). XPS quantification showed that the N 1s atomic concentration increased from 5.22 at% (PES) to 7.70 at% (PES-Pdop) and 10.17 at% (PES-Pdop-DNaseI), confirming stepwise surface functionalization and DNase I immobilization (Fig. S3(c)). A fluorophore-labeled DNase activity, measured at excitation/emission wavelengths of 535/565 nm using the assay kit, showed that the immobilized enzyme retained activity comparable to its free form as a control. Embedding this PES-Pdop-DNase I biocatalytic membrane into a 16 μL μ-TFF unit enabled one-step DNA template digestion and simultaneous removal of NTPs and salts under continuous flow.

A 3D-printed μ-TFF unit (internal volume ~16 μL) was fabricated as described in section 4.2 and is shown in Fig. S2(c). The DNA digestion performance of the μFD module was evaluated using a 7.5 μg FLuc DNA template, circulated through a 3 mm × 30 mm channel at a total flow rate of 100 μL min^{-1} (20 μL min^{-1} retentate, 80 μL min^{-1} permeate) (Fig. 2(a)). Complete digestion and removal of the DNA template were achieved within three recirculation cycles (<5 min total), as confirmed by agarose gel electrophoresis (AGE) (Fig. 2(b)). Lane 1 shows the untreated DNA template, lane 2 corresponds to one digestion cycle, lane 3 to two cycles, and lane 4 demonstrates complete digestion and clearance. The μFD module was further tested with crude IVT reaction mixtures (Fig. 2(c)), where it selectively degraded and removed the DNA template while retaining full-length mRNA.

To assess operational stability, the reusability of the DNase I-functionalized biocatalytic membrane was evaluated to be over five consecutive runs. The membrane maintained 98% of its initial digestion efficiency, indicating excellent durability, reusability, and enzymatic stability under continuous-flow conditions. To our knowledge, this is the first demonstration of an integrated biocatalytic μ-TFF unit (unit operation B) serving as a single, automated module that combines enzymatic digestion and selective separation. This configuration eliminates the need for discrete batch digestion and filtration steps, thereby streamlining downstream processing in mRNA therapeutics manufacturing.

2.4 Automated multimodal chromatography (MMC) module for mRNA purification

After DNA digestion and small-molecule removal in the μFD module (unit operation B), purification was carried out *via* an automated MMC step, which selectively captured and recovered full-length mRNA while removing residual T7 RNA polymerase and aberrant or truncated RNA species. A Python-scripted controller coordinated multi-valved syringe pumps to deliver all buffers, including equilibration, binding, wash, elution, and cleaning, at precisely defined flow rates (Fig. S4 and S5). Prior to each run, the program primed fluidic lines, verified valve positions, and calibrated in-line pH and conductivity sensors. Step transitions were governed by real-time sensor feedback rather than fixed timers: progression occurred only when pH and conductivity values entered predefined target ranges and remained stable across consecutive measurements. Throughout each run, valve states, flow rates, and pH/conductivity readings were time-stamped at 1–2 s intervals, enabling traceable data logging and minimizing operator-dependent variability (see section 4.4 for operational details and Fig. 3(a)). To balance productivity and recovery, the controller executed automated flowrate sweeps during load/wash/elution to identify Pareto-

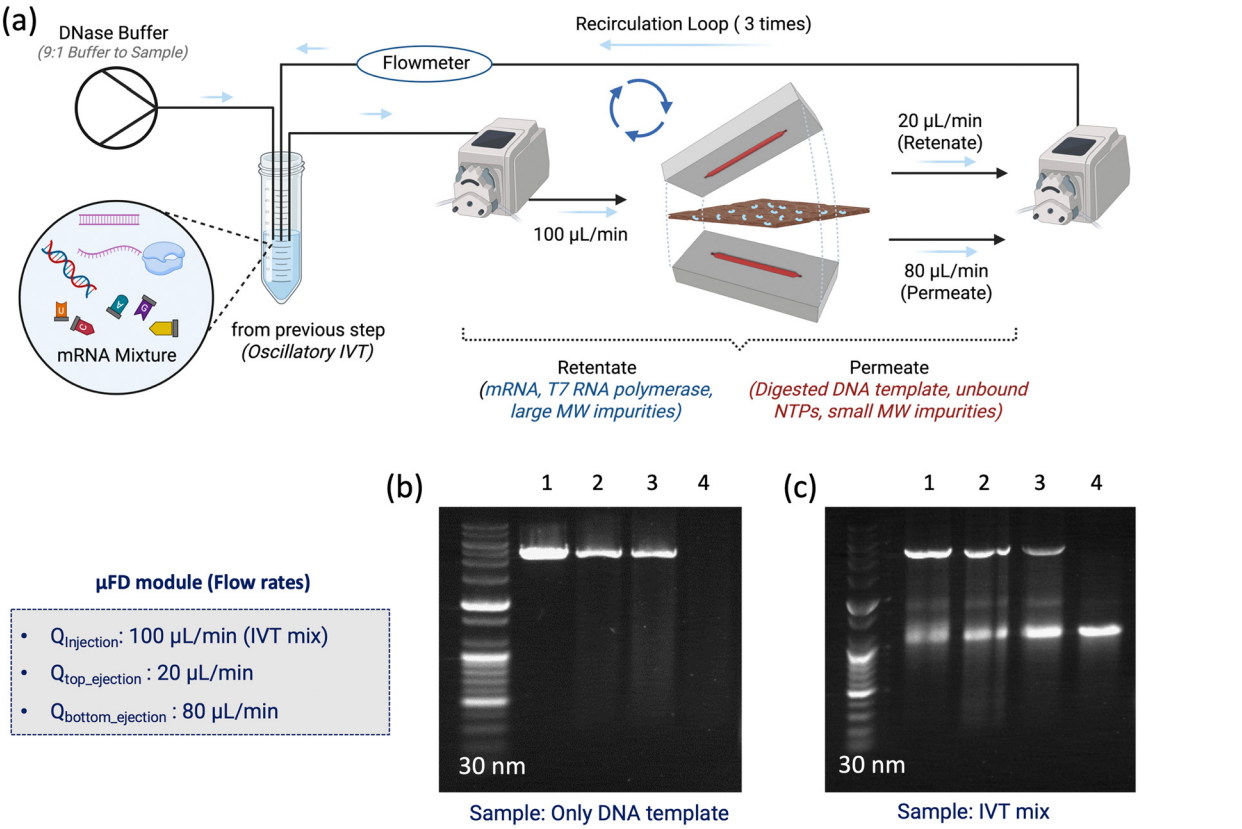

Fig. 2 Automated microfluidic digestion/clarification (µFD) module for inline DNA template digestion and clarification of the crude Os(IVT) product. (a) Schematic of the µFD module. (b) AGE analysis of DNA digestion using the PES-Pdop-DNase I membrane (only DNA template as sample). (c) Electrophoretic analysis of DNA digestion in the IVT mixture after sequential digestion cycles.

optimal conditions; under the optimized regime, recovery reached ~93.3% (see Fig. S5).

This closed-loop, sensor-driven approach enhanced clearance of truncated mRNA species and residual T7 RNA polymerase, improved run-to-run reproducibility, and reduced overall cycle times. Under the optimized regime, elution fractions yielded 93.3% mRNA recovery, as shown in Fig. S5. Integrity, concentration, and function of the purified mRNA were confirmed by UV-vis, denaturing AGE, *in vitro* translation, and ELISA-based dsRNA/T7 polymerase quantification, supporting suitability for therapeutic applications. Compared with oligo-dT capture, the MMC workflow delivered higher yield and purity (Table 1; Fig. 5). Finally, a 30 kDa MWCO hollow-fiber TFF module (HF-TFF, unit operation D), as demonstrated in Fig. 3(b), concentrated and buffer-exchanged the product, completing the downstream sequence. Overall, the automation framework, Python-orchestrated pumps/valves with pH-conductivity gating and event-driven step transitions, was pivotal in achieving high-resolution, reproducible purification.

2.5 Comparative evaluation of the discrete/sequential modular process

The efficiency of the mRNA synthesis and purification modules in discrete and sequential processing was validated through comparison with conventional batch-mode performance. The various sequential workflows across all combinations of discrete IVT, DNA digestion, and purification step were evaluated by comparing the results of mRNA yield and purity as follows:

- IVT of the FLuc DNA template: batch [B(IVT)] *vs.* oscillatory microfluidic [Os(IVT)] (section 2.2).
- DNA digestion: batch-mode DNase I [BD] *vs.* microfluidic TFF with PES-Pdop-DNase I [µFD] (section 2.3).
- Purification: oligo-dT affinity [OdT] *vs.* PrimaS multimodal chromatography [MMC] (section 2.4).

To compare overall workflow performance, total processing time was defined as the complete end-to-end duration of each workflow as implemented in this study, and productivity was determined by normalizing mRNA yield to total time. For discrete workflows, an additional 0.5 h was included to account for manual transfer and holding between modules (*i.e.*, collection, reconnection, and handling), whereas this additional time was not required for the integrated platform due to automated in-line routing between unit operations. As demonstrated in Table 1, the conventional process of a fully batch workflow, discrete B(IVT) + BD + OdT, yielded 641 ± 0.6 µg FLuc mRNA, whereas swapping OdT with MMC improved yield to 870 ± 2 µg with a comparable purity ($A_{260/230}$ = 2.14). It indicated the superior binding selectivity and capacity of the automated MMC step over conventional affinity purification.

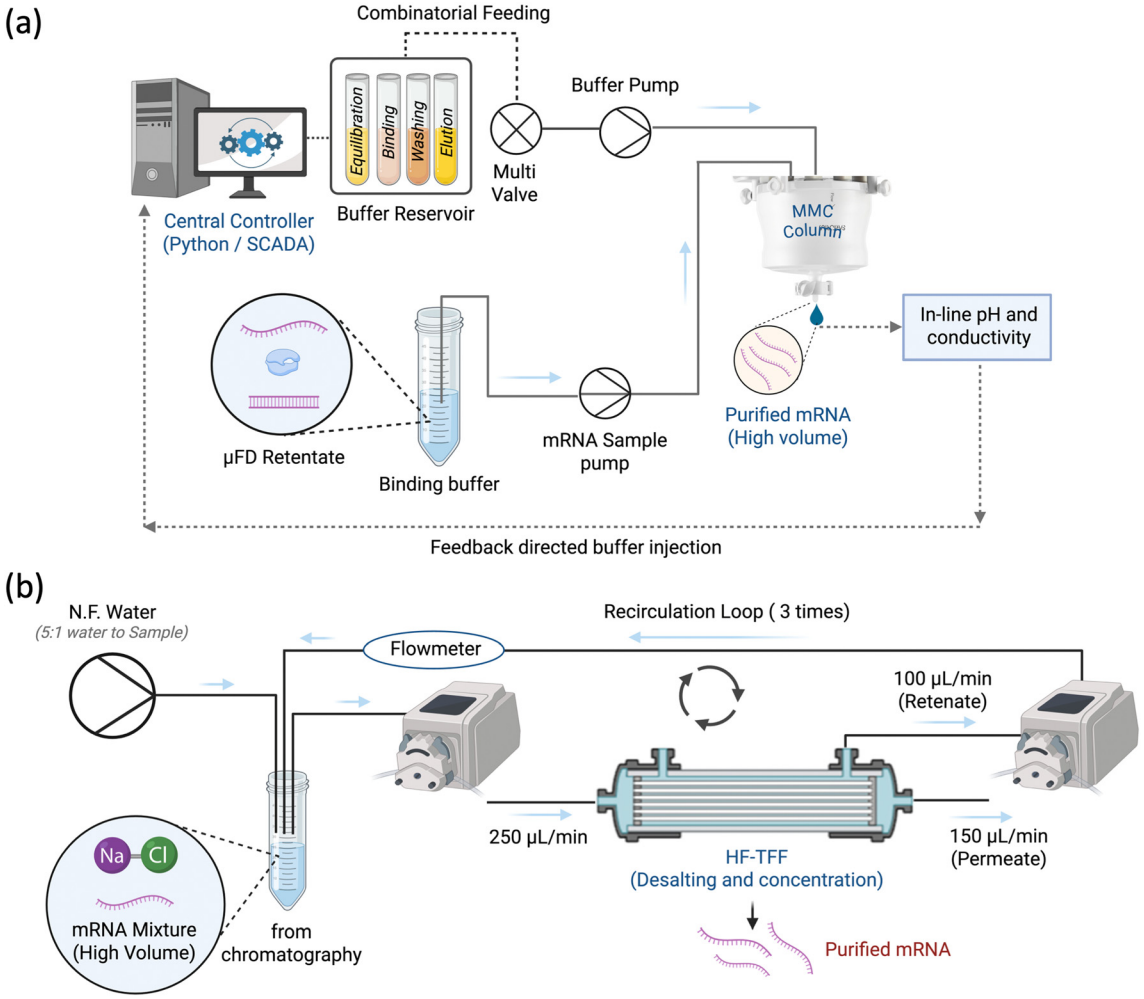

Fig. 3 Automated downstream processing modules for mRNA purification, desalting, and concentration, comprising (a) multimodal chromatography (MMC) and (b) hollow-fiber tangential flow filtration (HF-TFF).

Table 1 Comparison of mRNA yield, purity ($A_{260/230}$), processing time, and productivity between batch and automated microfluidic workflows. Abbreviations: Os(IVT), oscillatory *in vitro* transcription; B(IVT), batch *in vitro* transcription; BD, batch digestion; μFD, microfluidic digestion/clarification; MMC, multimodal chromatography; OdT, oligo(dT); FLuc, firefly luciferase; M1 and M2, modified nucleotide formulations 1 and 2, respectively; pGEM, pGEM-derived DNA template

Workflow	Modular process	DNA template-NTP	mRNA yield (μg)	Purity $A_{260/230}$	Productivity (μg·h^{-1})
Discrete	B(IVT) + BD + OdT	FLuc	641 ± 0.6	2.11	98.6
	B(IVT) + BD + MMC	FLuc	870 ± 2	2.14	133.8
		pGEM	1224 ± 2.1	2.09	188.3
		FLuc-M1	853.5 ± 0.6	2.11	131.3
		FLuc-M2	879 ± 0.5	2.19	135.2
	Os(IVT) + BD + OdT	FLuc	773 ± 0.6	2.20	309.2
	Os(IVT) + BD + MMC	FLuc	1241 ± 1.2	2.16	496.4
	Os(IVT) + μFD + OdT	FLuc	864 ± 1.5	2.25	345.6
	Os(IVT) + μFD + MMC	FLuc	1283 ± 1.3	2.27	513.2
Integrated	**[Os(IVT)–μFD–MMC]**	FLuc	1275 ± 1.7	2.26	637.5
		pGEM	1315 ± 2.8	2.33	657.5
		FLuc-M1	1254 ± 1.1	2.26	627.0
		FLuc-M2	1262 ± 0.6	2.31	631.0

Os(IVT) of the discrete Os(IVT) + BD + OdT workflow boosted yield to 773 ± 0.6 μg with better purity ($A_{260/230}$ = 2.20), a 21% gain over the equivalent B(IVT) workflow. Notably, double micromixers enhanced enzyme–substrate interactions at precise

control of mixing and residence time.[25] Moreover, combining Os(IVT) with MMC in the discrete Os(IVT) + BD + MMC workflow nearly doubled batch-based yield to 1241 ± 1.2 μg (94% increase). Finally, replacing BD with the μFD module in the discrete Os(IVT) + μFD + MMC workflow delivered the highest yield (1283 ± 1.3 μg) and highest purity ($A_{260/230}$ = 2.27). To directly compare capture-step performance under identical upstream conditions, the Os(IVT) + μFD material was purified using MMC and oligo-dT affinity capture. MMC increased mRNA recovery from 864 ± 1.5 μg (Os(IVT) + μFD + OdT) to 1283 ± 1.3 μg (Os(IVT) + μFD + MMC), corresponding to an approximately 1.5-fold (~48.5%) improvement, while maintaining comparable UV purity ($A_{260/230}$ = 2.25 for OdT *vs.* 2.27 for MMC) (Table 1). Incorporation of μFD upstream supported capture performance by reducing the DNA/impurity load prior to purification; this is particularly relevant because residual or fragmented template DNA, like mRNA, can contribute to competitive interactions in nucleic-acid separations and increase fouling/overloading risks during capture. The observed recovery difference is therefore primarily attributable to the capture mechanism: oligo-dT relies on poly(A) hybridization and is more sensitive to poly(A) accessibility/secondary structure as well as bead-based capacity and mass-transfer limitations, which can increase losses during binding, washing, and elution. In contrast, MMC provides convective monolith capture with combined electrostatic/hydrophobic interactions and automated, sensor-gated operation, which is more tolerant to crude feeds and can reduce handling-related losses and operator-dependent variability. Importantly, the similar $A_{260/230}$ values indicate that the higher recovery achieved with MMC is obtained without compromising overall purity. This strategic step improved process selectivity and streamlined purification, minimizing loss and enhancing purity, indicating the individual contributions of each step. It is known that the co-presence of negatively charged DNA and mRNA hindered mRNA adsorption efficiency due to competitive binding interaction.[3,21] Pre-removal of DNA in the single step μFD process was critical to prevent binding site competition, improve the specificity of MMC, and eliminate residual enzyme carryover. Immobilization of DNase I on the membrane also enhanced both enzyme stability and reusability.[23] Collectively, the discrete and continuous process of the Os(IVT) + μFD + MMC sequence enables efficient microfluidic transcription, inline DNA digestion, and high-resolution mRNA purification, establishing a foundation for a fully automated, continuous mRNA manufacturing platform.

2.6 Integrated mRNA synthesis and purification of the automated microfluidic platform

By leveraging superior performance in the mRNA yield and purity achieved by the discrete and sequential Os(IVT) + μFD + MMC workflow, a fully integrated microfluidic platform, [Os(IVT)–μFD–MMC], was developed to streamline the flow process. This platform connects four modules (Fig. 4): Os(IVT), μFD, automated MMC, and a final HF-TFF module. This

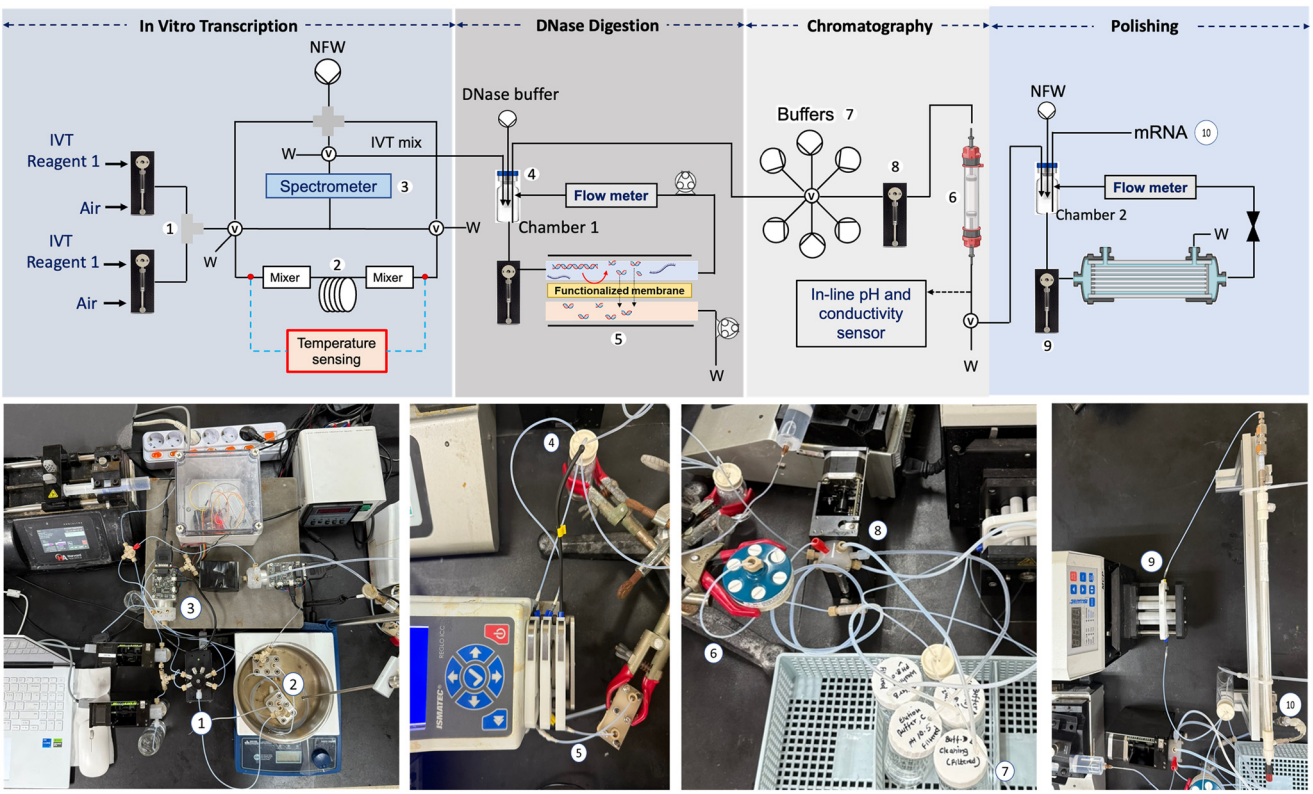

Fig. 4 Integrated automated microfluidic platform for end-to-end mRNA synthesis, digestion/clarification, and purification. The labels correspond to: (1) multi-valve pump, (2) IVT reaction zone, (3) spectrometer, (4) collection vial for the IVT outlet, (5) μFD unit, (6) MMC column, (7) buffer set, (8) multi-valve pump for the chromatography steps, (9) pump for the HF-TFF step, and (10) purified mRNA.

modular configuration enables quasi-continuous processing through automated reagent delivery, in-line purification, and seamless interfacing between unit operations, ensuring high-yield and high-purity mRNA production.

The core components of the Os(IVT) module, including two PTFE serpentine micromixers positioned at either end of the 3.8 m capillary reactor, a precision segment-injection manifold, valve array, in-line spectrometer, and syringe-pump controllers, are consistently maintained across both the standalone and integrated configurations. To incorporate the Os(IVT) module into a streamlined mRNA manufacturing pipeline, the integrated platform utilizes GMP-compliant, quick-connect ports, enabling direct linkage to upstream IVT reagent feed tanks and downstream purification modules. Initially, the controller leads to form a five-segment plug by feeding precise doses of IVT solutions, air and NFW in a stepwise manner as aforementioned (Fig. S1), injects it into the micromixer and reaction zone under oscillatory flow, and uses optical feedback to trigger flow reversal. Upon reaching the target reaction time, the crude IVT mixture is routed to a collection chamber. Subsequently, the controller dilutes the IVT mixture with DNase buffer and feeds it into the μFD module. Flow partitioning (retentate/permeate) and cycle count are executed automatically, as detailed in section 2.3. Event-driven gating terminates digestion after three cycles. Within 5 min, the DNA template and smaller impurities are removed, and the process proceeds to chromatography.

The entire end-to-end workflow of the integrated platform is orchestrated by a centralized SCADA/MES layer (supervisory control and data acquisition/manufacturing execution system) that, implemented in Python, replaces individual module graphical user interfaces (GUIs). This control layer schedules Os(IVT) plug injections; regulates reagent delivery, flow direction, step-specific flow rates, and buffer compositions; and routes fractions *via* programmable valves to designated collection chambers. The controller automates column equilibration, sample dilution in binding buffer, loading, washing, and elution. Real-time measurements from process-connected probes provide continuous pH and conductivity feedback, which trigger step transitions and alarms. The same control layer also automates cleaning-in-place (CIP) and sterilization-in-place (SIP) procedures between runs. The system is re-equilibrated using enforced valve states and residence times, ensuring consistent cycle-to-cycle performance. Notably, each unit operation is hard-linked to the next, ensuring uninterrupted streamline-flow throughout the process. Final pooled fractions are concentrated and buffer-exchanged using a 30 kDa HF-TFF module. All operations are logged at 1–2 s intervals. The closed, cleanable fluidic path minimizes contamination risk and simplifies turnaround between runs.

As seen in Table 1, the integrated workflow consistently produced mRNA with high yield (1275 ± 1.7 μg) and purity ($A_{260/230}$ = 2.26), comparable to those achieved by discrete and sequential workflows. Notably, FLuc mRNA protein expression was enhanced significantly compared to the batch process (Fig. 5d), surpassing previous results obtained using Os(IVT) and LiCl precipitation.[25] These findings demonstrate that the integrated platform operates seamlessly under optimized conditions, maintaining equivalent performance in both yield and purity. As previously noted, the robust performance of both integrated and discrete workflows, comprising Os(IVT), μFD, and MMC modules, confirms that the integrated system preserves the optimized functionality of each module while enabling fully automated operation, underscoring its precision and reproducibility. To consolidate the system performance, mRNA synthesis and purification is extensively adopted to a different DNA template (pGEM) and nucleotide compositions *i.e.*, non-modified (NM) and modified N^1-methyl-pseudo-UTP (FLuc-M1), N^6-methyl-ATP (FLuc-M2) with FLuc template DNA, summarized in Fig. 5(d) and Table 1 (Fig. S6 and S7). Using the pGEM template with NM nucleotides, the integrated system achieved 1314 ± 2.8 μg mRNA with a purity of 2.33 ($A_{260/230}$), compared to 1224 ± 2.1 μg and 2.09 ($A_{260/230}$) in batch mode. This demonstrates the platform's adaptability to different gene templates, regardless of sequence length or complexity. The continuous-flow design minimizes hold-up volume and sample loss, contributing to superior process fidelity. The platform also showed compatibility with chemically modified nucleotides. With N^1-methyl-pseudo-UTP, the integrated setup produced 1253.5 ± 1.1 μg mRNA (purity 2.26), compared to 833.5 ± 0.6 μg ($A_{260/230}$ = 2.11) in batch mode. For N^6-methyl-ATP, the integrated system yielded 1261.5 ± 0.6 μg ($A_{260/230}$ = 2.31), outperforming the batch result of 879 ± 0.5 μg ($A_{260/230}$ = 2.19).

In the integrated platform, the Os(IVT) module enhances transcription efficiency through rapid, uniform mixing and precise residence-time control, while maintaining tight temperature regulation in small volumes. These homogeneous reaction conditions suppress off-pathway events and minimize dsRNA formation at the source. The μFD module enables simultaneous template DNA degradation and tangential removal of fragments within 5 min, eliminates free-enzyme carryover, facilitates inline salt removal in a closed system, and improves downstream chromatography performance by preventing DNA–mRNA competition. The automated MMC step leverages dual interaction modes to achieve high selectivity and short cycle times. Event-driven pH and conductivity gating, combined with automated flow-rate sweeps, identify Pareto-optimal conditions for loading, washing, and elution, resulting in high recovery (~93%) and effective removal of truncated RNAs and residual T7 polymerase. The final step is performed *via* HF-TFF, which gently and reproducibly concentrates and buffer-exchanges the product under automation-gated volume endpoints, preserving mRNA integrity. Collectively, this integrated, closed-loop control architecture shortens total cycle time (~2 h per run), facilitates straightforward scale-up *via* extended operation or parallelization, and delivers superior product quality alongside improved yield and throughput. The inclusion of process time and productivity metrics in Table 1 enables direct comparison across discrete workflows and the integrated platform, highlighting the throughput gains achieved through automation and module integration. The total processing time for each workflow was calculated by summing

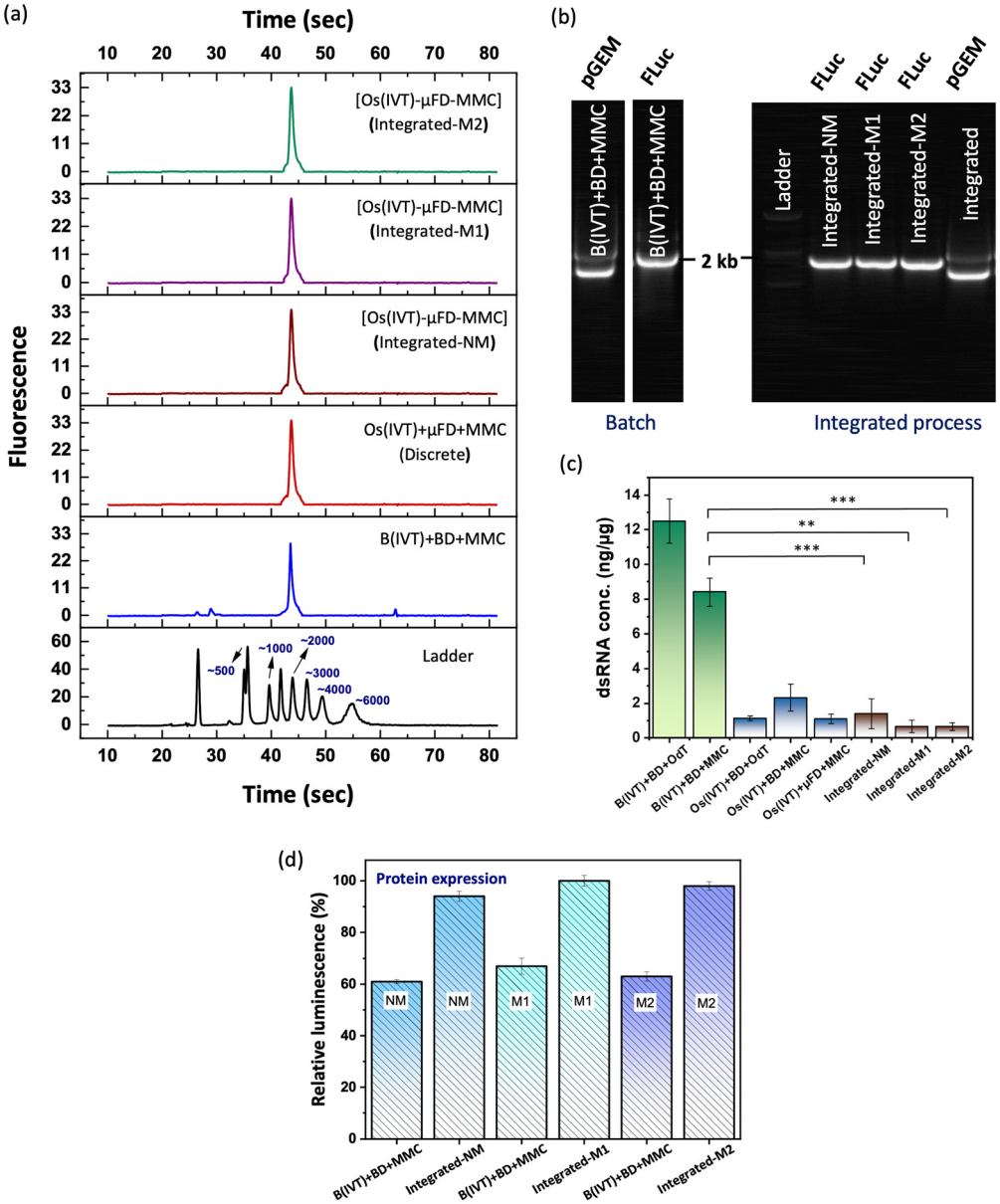

Fig. 5 Performance of the integrated [Os(IVT)–μFD–MMC] workflow in improving mRNA quality and functional activity. (a) CE profiles of purified mRNA after downstream processing. (b) Denaturing AGE analysis of full-length mRNA integrity across workflows. (c) dsRNA impurity analysis by ELISA (rJ2); (d) functional expression of FLuc mRNA in HeLa 229 cells for batch and integrated workflows (NM, M1, and M2), reported as batch-normalized relative luminescence units (RLU). Data are mean ± SD (n = 3). Statistical significance was assessed by two-way ANOVA with Tukey's multiple-comparisons test ($p < 0.05$).

the programmed durations of the constituent unit operations. For batch workflows, total time was calculated from the batch IVT reaction, digestion, and downstream purification steps (OdT or MMC, and concentration), yielding an overall end-to-end duration of ~6 h as implemented in this study. For microfluidic workflows, this included Os(IVT) (1.0 h), μFD digestion/clarification (<0.1 h), capture purification by MMC (<0.5 h) or oligo-dT (0.5 h), and HF-TFF concentration/buffer exchange (~0.5 h), with an additional 0.5 h included for discrete workflows to account for manual transfer/holding between modules. Therefore, it envisions that the resulting workflow consistently produces drug-substance grade mRNA suitable for downstream formulation in vaccines and RNA-based therapeutics.

2.7 mRNA integrity and impurity profiling across different processes

Regulatory authorities such as the FDA and EMA mandate comprehensive quality characterization of therapeutic mRNA products to ensure safety and efficacy.[28] To address these requirements, mRNA samples produced *via* batch, discrete, and integrated workflows were systematically analyzed for transcript

integrity, sequence length, and IVT-derived impurities, including dsRNA and residual T7 RNA polymerase.

Transcript integrity and sequence length. The structural integrity of FLuc mRNA was assessed using the LabChip GXII Touch System, a high-resolution capillary electrophoresis (CE) platform capable of distinguishing full-length transcripts from truncated or degraded species. This analysis is critical, as intact transcripts are essential for optimal translation and therapeutic performance, whereas fragmented RNA may compromise efficacy and provoke unintended immune responses.[29] As shown in Fig. 5(a), electropherograms revealed that batch workflow B(IVT) + BD + MMC exhibited secondary peaks in the 25–30 s range, indicative of truncated or aberrant transcripts. In contrast, samples generated *via* the integrated [Os(IVT)–μFD–MMC] workflow of NM, M1 and M2 displayed a singular, sharp peak at ~43 s, corresponding to a ~1960 nucleotide transcript, consistent with the expected length of full-length FLuc mRNA. These findings were corroborated by denaturing AGE (Fig. 5(b)), which showed distinct bands around 2 kb for integrated samples, thereby confirming transcript integrity and sequence length.

Quantification of dsRNA impurities. dsRNA, a known immunostimulatory byproduct of IVT, was quantified using J2 monoclonal antibody-based ELISA and dot-blot assays. As depicted in Fig. 5(c) and S8, batch-derived mRNA contained dsRNA concentrations ranging from 8–12 ng μg^{-1} mRNA. In contrast, the integrated microfluidic process consistently reduced dsRNA levels to below 3 ng μg^{-1} mRNA. This reduction not only enhances the safety profile of the final product but also minimizes the burden on downstream purification steps and lowers overall production costs.[30] The integrated platform achieved 83.3% reduction in dsRNA relative to the batch process [B(IVT) + BD + MMC], representing a 65% improvement over the previous benchmark.[25] Moreover, comparable reductions were also observed in samples incorporating chemically modified nucleotides, validating the robustness of the integrated platform (Fig. 5(c)).

Residual T7 RNA polymerase detection. Residual T7 RNA polymerase, an IVT enzyme with potential immunogenicity, was evaluated using an anti-T7 RNA polymerase ELISA kit. Both batch and integrated workflows effectively eliminated residual enzyme during the MMC step, with levels falling below the detection threshold, thereby meeting regulatory purity standards.[7] Collectively, the data presented in Fig. 6 demonstrate that the integrated microfluidic workflow enables the production of structurally intact, full-length mRNA with significantly reduced impurity profiles. This platform offers a scalable and regulatory-compliant solution for the manufacturing of high-quality mRNA therapeutics.

The integrated [Os(IVT)–μFD–MMC] workflow improves mRNA quality and functional performance. (a) Capillary electrophoresis (CE) profiles of purified mRNA showing enrichment of full-length transcript and removal of low-molecular-weight species after downstream processing. (b) Denaturing agarose gel electrophoresis (AGE) confirming ~2 kb full-length mRNA integrity across workflows. (c) dsRNA impurity analysis by ELISA and dot blot (rJ2) demonstrating reduced dsRNA in the integrated workflow; representative dot blot images are provided in the SI (Fig. S8). (d) Functional expression of FLuc mRNA in HeLa 229 cells for batch and integrated workflows (NM, M1, M2 as defined in the text), reported as relative luminescence units (RLU) normalized to the batch condition. Data are mean ± SD (n = 3); statistical significance was assessed by two-way ANOVA followed by Tukey's multiple-comparisons test, with $p < 0.05$ considered significant.

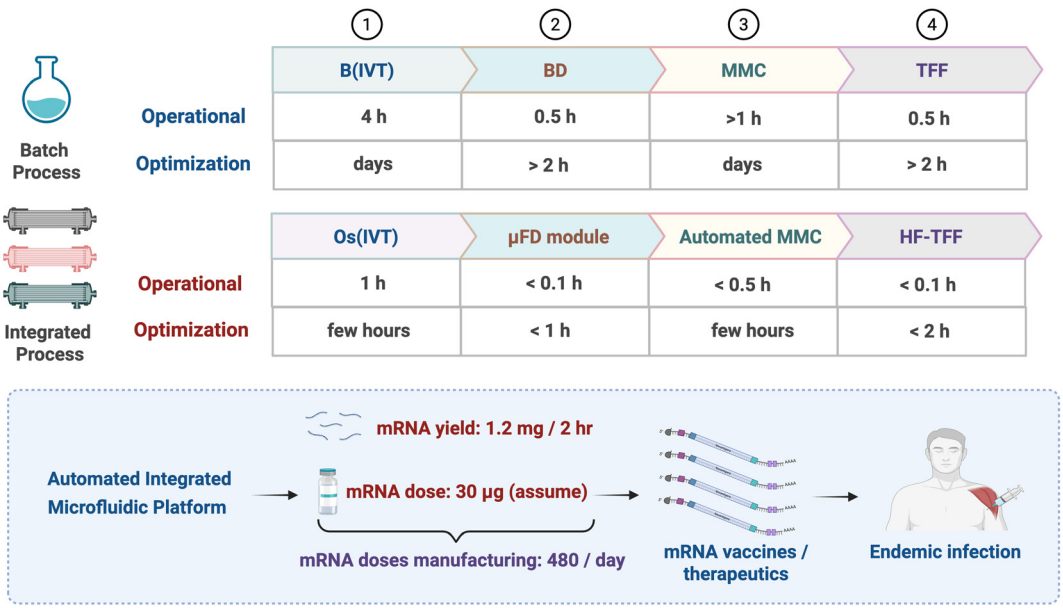

Fig. 6 Operational sequence, processing timeline, and productivity analysis of the integrated automated microfluidic platform for mRNA manufacturing.

2.8 Performance evaluation of the integrated mRNA manufacturing platform

The integrated platform consolidates IVT, template digestion/clarification, capture, and concentration into a quasi-continuous, automated sequence that reduces end-to-end processing time from ~6 h in the conventional batch workflow (IVT 4 h; digestion ~0.5 h; capture ≥1 h; concentration ~0.5 h) to ~2 h (Os(IVT) 1 h; μFD <0.1 h; automated MMC <0.5 h; HF-TFF <0.1 h). Beyond speed, the integrated runs delivered consistently high mRNA quality, enhanced translational efficiency, lower dsRNA, and minimal truncated species, owing to closed-loop control and in-line pH/conductivity monitoring during purification. Using experimentally validated outputs, the integrated platform produced 1275 ± 1.7 μg mRNA per run in ~2 h, representing a bench-scale, research- to preclinical-scale production level suitable for process development and small-scale biological evaluation. For perspective, this output corresponds illustratively to ~40 doses only if a 30 μg dose is assumed; however, actual dose requirements vary substantially with the mRNA product, formulation, and clinical indication. Higher production capacity could be achieved by extended operation or numbering-up of the modular workflow. Quantitatively, the integrated workflow produced 1275 ± 1.7 μg mRNA per run ($A_{260/230}$ = 2.26) compared with 641 ± 0.6 μg for the fully batch benchmark B(IVT) + BD + OdT ($A_{260/230}$ = 2.24), corresponding to an ~2.0× increase in end-to-end yield (Table 1), while maintaining robustness across DNA templates and nucleotide chemistries. To support scalability, the architecture is compatible with "number-up" parallelization of Os(IVT) channels with uninterrupted transfer into μFD → MMC → HF-TFF, reducing hold times and manual transfers. Together, these results establish the platform's ability to deliver stable output quality with markedly reduced cycle time and compact footprint suitable for decentralized or rapid response manufacturing (Fig. 6).

The time reduction in downstream purification arises from three factors. First, the μFD module combines DNase I digestion and clarification in a single continuous step; complete template removal is achieved within <5 min across three short recirculation loops, eliminating a 30 min batch incubation and the subsequent transfer/hold. Second, the automated MMC uses sensor-gated step transitions, progressing only when pH and conductivity enter set ranges, so the controller avoids fixed, overlong waits and terminates wash/elution at plateaus, shortening cycle times while maintaining recovery (~93%). Finally, the HF-TFF is run to automation-gated volume endpoints, preventing unnecessary over-concentration steps, and the closed path removes manual transfer delays and re-setups between units (see Fig. S4 and S5 for the automated purification steps).

The integrated design enables seamless, automated transfer of the product stream through a closed, sterile fluidic path, effectively mitigating RNase contamination and eliminating product loss associated with manual batch transfers. Notably, automated operation with real-time analysis also significantly accelerates the optimization process by compromising complex parameters. The modular architecture of the microfluidic platform supports straightforward scalability *via* numbering-up of individual unit operations, preserving process efficiency, reproducibility, and operational consistency.[31] Incorporation of single-use technologies further reduces operational complexity and cost by eliminating the need for repeated sterilization, enhancing the platform's economic feasibility for commercial-scale manufacturing.[32] Moreover, the system's versatility allows future expansion toward advanced RNA modalities, such as self-amplifying mRNA (saRNA) and miRNA sponge-based therapeutics. Integration of engineered RNA polymerases with enhanced fidelity, developed through directed evolution and high-throughput screening, could further improve IVT performance and reliability. Finally, coupling the platform with advanced analytical instrumentation and artificial intelligence (AI)-driven process optimization would enable real-time monitoring and adaptive control, enhancing responsiveness to evolving therapeutic demands and further elevating manufacturing efficiency.

3. Conclusions

We report a centrally computer-controlled, modular microfluidic platform that integrates key unit operations for end-to-end mRNA synthesis and purification. The workflow combines an (Os(IVT)) module for intensified transcription, a microfluidic digestion/clarification (μFD) module incorporating a DNase I-immobilized biocatalytic membrane with inline micro-TFF for rapid template removal and buffer exchange, and an automated multimodal chromatography (MMC) module with in-line pH and conductivity monitoring for reproducible capture and elution. Together, these modules form a unified [Os(IVT)–μFD–MMC] process that reduces manual handling and enables seamless transfer between unit operations under software control. Using FLuc mRNA as a model, the integrated platform completed synthesis-to-purification in 2 h and produced 1275 ± 1.7 μg (~1.2 mg) mRNA per run, compared with 641 ± 0.6 μg for the fully batch benchmark B(IVT) + BD + OdT (~2.0×), while the MMC step achieved ~93.3% recovery under optimized operation. The platform-maintained transcript integrity (full-length ~2 kb) and improved functional performance, consistent elevated translation after integration relative to the batch workflow. Importantly, dsRNA impurities were reduced by 83.3%, supporting improved product quality alongside higher yield and productivity. The platform also demonstrated adaptability across different templates (*e.g.*, pGEM) and nucleotide compositions, highlighting its utility for rapid process development and modular reconfiguration. Overall, this work advances oscillatory microfluidic IVT from a standalone intensified reactor to an automated, end-to-end lab-on-a-chip workflow that integrates enzymatic processing, filtration-based conditioning, and sensor-guided chromatographic purification. The approach provides a compact foundation for scalable operation *via* extended runtime or numbering-up, and offers a practical route toward

reproducible, high-quality mRNA production in settings where speed, flexibility, and reduced operator dependence are critical.

4. Experimental section

4.1 Materials

Firefly luciferase (FLuc) DNA template and SmartCap cap analog were donated by ST Pharm Co. (Republic of Korea). T7 RNA polymerase, nucleotide triphosphates (NTPs) and RNase inhibitor were purchased from Enzynomics Co. (Republic of Korea). DNase I, lithium chloride (LiCl) and Dynabeads™ oligo-dT were purchased from Thermo Fisher Scientific (USA). Agarose and MOPS buffer were purchased from Bioneer Corp. (Republic of Korea). Formaldehyde (37%), DMSO, DTT and HRP-conjugated secondary antibody were purchased from Sigma-Aldrich (USA). Rabbit reticulocyte lysate and luciferase assay systems were purchased from Promega (USA). HeLa 229 cells (RRID: CVCL_0030; KCLB, Korea) were mycoplasma-free. Anti-dsRNA antibody (clone rJ2) was purchased from Jena Bioscience (Germany). A T7 RNA polymerase ELISA kit was donated by Hzymes Biotechnology (China). PTFE tubing (I.D. 1 mm, O.D. 1.6 mm) was purchased from Revodix (Republic of Korea). UV-curable resin (Plas.CLEAR v2.0) was purchased from ASIGA (Australia). For μFD, a hydrophilic PES membrane (0.03 μm pore size; GVS, cat. no. 1235748) was used. For the HF-TFF step, a MiniLab hollow fiber module (Membrane Solutions, HFEMN030050320; 30 kDa MWCO mPES; 30 cm^2) was used. All solutions were prepared in nuclease-free water. Unless otherwise stated, experiments were performed in triplicate and data are reported as mean ± SD.

4.2 IVT stock solutions and oscillatory IVT operation (Os(IVT))

IVT was performed in batch and oscillatory configurations using two stock solutions (Table S1). Solution 1 contained the linearized FLuc DNA template, NTPs, and cap analog; solution 2 contained T7 RNA polymerase and transcription buffer. Yeast inorganic pyrophosphatase (1 U μL^{-1}) and RNase inhibitor were included. In Os(IVT), a total reaction volume of 150 μL was formed by 1 : 1 co-injection of the two solutions (75 μL each) as a segmented plug. The plug was oscillated through PTFE serpentine micromixers (5 cm length, 500 μm × 500 μm cross-section) and a capillary reactor (3.8 m) with in-line spectrometer feedback to trigger valve switching and flow reversal (Fig. S1). Unless stated otherwise, Os(IVT) used a micromixer flow of 1 mL min^{-1} and capillary flow of 100 μL min^{-1} to provide a 60 min residence time at 37 °C (see Table S1 for compositions). mRNA was resuspended in nuclease-free water and quantified by A_{260} (NanoDrop 2000c, Thermo Fisher Scientific). Device fabrication/assembly details are provided in Method S1.

4.3 μFD module: DNase-immobilized biocatalytic membrane with micro-TFF clarification

A hydrophilic PES membrane (0.03 μm pore size) was functionalized with a polydopamine (PDA/Pdop) layer and used for DNase I immobilization to enable inline template digestion in a micro-TFF configuration. The μTFF device (internal volume ~16 μL) was fabricated by DLP printing and post-cured under UV irradiation; device geometry and dimensions are provided in Fig. S2. Membrane pore size selection and surface characterization (contact angle, XPS) are provided in Fig. S3. For μFD operation, template digestion/clarification was performed using retentate/permeate flow partitioning of 20/80 μL min^{-1} (total 100 μL min^{-1}) over three short recirculation cycles (<5 min total), which achieved complete template digestion/removal while retaining full-length mRNA in the retentate (Results, Fig. 3). Detailed membrane functionalization/immobilization protocols, μTFF fabrication, and activity/characterization data are provided in the SI (Fig. S2 and S3; Method S2).

4.4 Automated multimodal chromatography (MMC) under sensor-gated control

Purification was performed using a CIMmultus PrimaS 1 mL monolith under a Python-scripted automation layer coordinating syringe pumps/valves and in-line pH and conductivity sensing. Before each run, the controller primed lines, verified valve states, and calibrated pH/conductivity probes. Step transitions (equilibration → load → wash → elution) were event-driven: progression occurred only when pH and conductivity entered predefined target ranges and stabilized across consecutive measurements. All valve states, flow rates and sensor readings were logged every 1–2 s.

The column was equilibrated with Buffer A (20 mM Tris-HCl, pH 8.0) at 5 mL min^{-1}. The μFD-treated IVT mixture was conditioned into buffer A and loaded at 1 mL min^{-1}. A low-salt wash used buffer B (20 mM Tris-HCl, 0.25 M NaCl, pH 8.0) until conductivity reached a plateau. Elution used buffer C (20 mM CAPS, 1 M NaCl, pH 10.5); fractions were collected within a predefined pH/conductivity "elution window". Automated CIP was performed after each run using NaOH/NaCl followed by re-equilibration in potassium acetate buffer (pH 5.5). MMC step programming diagrams and representative elution traces are provided in SI, Fig. S4 and S5; CIP/SIP concept in SI text.

4.5 Oligo-dT purification

For benchmark purification, Dynabeads™ oligo-dT capture was performed using LiCl binding buffer (20 mM Tris-HCl, pH 7.5, 1.0 M LiCl, 2 mM EDTA) with heat denaturation (65 °C, 2 min), binding, magnetic separation, washing, and water elution (Method S3: Oligo-dT purification protocol).

4.6 Integrity testing and translation efficiency

RNA concentration was determined by A_{260} ($1A_{260}$ = 40 μg mL^{-1} ssRNA) and purity was assessed by $A_{260/230}$. Transcript integrity/length was evaluated by denaturing agarose gel electrophoresis (1% agarose in MOPS/formaldehyde), with 0.5 μg RNA loaded per lane and electrophoresis at 50 V prior to imaging. Functional translation was assessed by (i) rabbit reticulocyte lysate *in vitro* translation (1 μg mRNA; 30 °C; 90

min) followed by luciferase readout, and (ii) HeLa 229 transfection (1 μg mRNA per well in 24-well plates; 48 h) followed by luciferase assay (Hidex Sense plate reader) (Method S3).

4.7 dsRNA and residual T7 RNA polymerase

dsRNA was assessed by dot blot using a positively charged nylon membrane, clone rJ2 antibody (1 : 5000), HRP-secondary antibody (1 : 10 000), chemiluminescence detection and ImageJ densitometry. dsRNA and residual T7 RNA polymerase were quantified by ELISA kits following manufacturer protocols (Fig. S8).

4.8 Integrated platform operation (quasi-continuous workflow)

The integrated [Os(IVT)–μFD–MMC] configuration hard-links the modules under a centralized Python SCADA/MES control layer that schedules Os(IVT) plug injection, executes μFD cycle counts and flow partitioning, runs sensor-gated MMC steps with automated CIP/SIP and re-equilibration, and performs HF-TFF for concentration (30 kDa MWCO; 30 cm^2). Representative operating settings were: Os(IVT) with 1 mL min^{-1} micromixer flow and 100 μL min^{-1} capillary flow (60 min residence at 37 °C); μFD using a 30 nm PES-Pdop-DNase I membrane with 20/80 μL min^{-1} retentate/permeate splitting over three short recirculation cycles (<5 min total); MMC using pH/conductivity-gated elution windows; and HF-TFF to automation-gated endpoints.

Platform adaptability was evaluated using the pGEM DNA template and modified nucleotides (N^1-methyl-pseudo-UTP and N^6-methyl-ATP). Discrete workflows (*e.g.*, B(IVT) + BD + OdT; Os(IVT) + BD + MMC; Os(IVT) + μFD + MMC) were executed as comparators as summarized in Table 1; template/nucleotide summary and yield comparisons are provided in Fig. S6 and S7.

Author contributions

Vikas Sharma: conceptualization, methodology, investigation, data curation, writing – original draft. Amirreza Mottafegh: methodology, investigation, data curation, writing – original draft. Jeong-Un Joo: conceptualization, investigation, data curation. Dong-Pyo Kim: conceptualization, project administration, funding acquisition, supervision, writing – review and editing.

Conflicts of interest

The authors declare that they have no known competing financial interests.

Data availability

The data that support the findings of this study are available on request from the corresponding author.

Supplementary information (SI): additional figures, experimental details and supporting analyses. See DOI: https://doi.org/10.1039/d6lc00118a.

Acknowledgements

We gratefully acknowledge the support from the National Research Foundation (NRF) of Korea grant funded by the Korean government (NRF-2017R1A3B1023598).

References

1 M. D. C. P. Royo, T. Arnold, I. P. Rodriguez, N. Ostrovsky, M. Al-Jazrawe, A. Hatas, A. S. Myerson and R. D. Braatz, *Sep. Purif. Technol.*, 2025, 134837, DOI: 10.1016/j.seppur.2025.134837.
2 S. S. Rosa, D. M. F. Prazeres, A. M. Azevedo and M. P. Marques, *Vaccine*, 2021, **39**, 2190–2200, DOI: 10.1016/j.vaccine.2021.03.038.
3 I. Choi, G. Y. Ahn, E. S. Kim, S. H. Hwang, H. J. Park, S. Yoon, J. Lee, Y. Cho, J. H. Nam and S. W. Choi, *Nano Lett.*, 2023, **23**, 7897–7905, DOI: 10.1021/acs.nanolett.3c01699.
4 J. Skok, P. Megušar, T. Vodopivec, D. Pregeljc, N. Mencin, M. Korenč, A. Krušič, A. M. Celjar, N. Pavlin, J. Krušič and M. Mueller, *Chem. Ing. Tech.*, 2022, **94**, 1928–1935, DOI: 10.1002/cite.202200133.
5 P. Vervaeke, S. E. Borgos, N. N. Sanders and F. Combes, *Adv. Drug Delivery Rev.*, 2022, **184**, 114236, DOI: 10.1016/j.addr.2022.114236.
6 J. Wegner, S. Ceylan and A. Kirschning, *Adv. Synth. Catal.*, 2012, **354**, 17–57, DOI: 10.1002/adsc.201100584.
7 J. Whitley, C. Zwolinski, C. Denis, M. Maughan, L. Hayles, D. Clarke, M. Snare, H. Liao, S. Chiou, T. Marmura and H. Zoeller, *Transl. Res.*, 2022, **242**, 38–55, DOI: 10.1016/j.trsl.2021.11.009.
8 L. Arnold, K. Lee, J. Rucker-Pezzini and J. H. Lee, *Biotechnol. J.*, 2019, **14**, 1800061, DOI: 10.1002/biot.201800061.
9 J. Hummel, M. Pagkaliwangan, X. Gjoka, T. Davidovits, R. Stock, T. Ransohoff, R. Gantier and M. Schofield, *Biotechnol. J.*, 2019, **14**, 1700665, DOI: 10.1002/biot.201700665.
10 J. Coffman, M. Brower, L. Connell-Crowley, S. Deldari, S. S. Farid, B. Horowski, U. Patil, D. Pollard, M. Qadan, S. Rose and E. Schaefer, *Biotechnol. Bioeng.*, 2021, **118**, 1735–1749, DOI: 10.1002/bit.27690.
11 M. N. São Pedro, T. C. Silva, R. Patil and M. Ottens, *Biotechnol. Bioeng.*, 2021, **118**, 3275–3286, DOI: 10.1002/bit.27757.
12 M. A. Wahab, C. Domingues, A. M. Azevedo, V. Chu, J. P. Conde and M. R. Aires-Barros, *Sep. Purif. Technol.*, 2024, **332**, 125702, DOI: 10.1016/j.seppur.2023.125702.
13 H. Mahal, H. Branton and S. S. Farid, *Biotechnol. Bioeng.*, 2021, **118**, 3468–3485, DOI: 10.1002/bit.27774.
14 A. Hengelbrock, A. Schmidt and J. Strube, *ACS Omega*, 2024, **9**, 8204–8220, DOI: 10.1021/acsomega.3c08732.
15 S. A. Kawale, D. C. Kang, G. N. Ahn, A. Mottafegh, J. H. Kang, G. S. Na and D. P. Kim, *Chem. Eng. J.*, 2023, **477**, 147033, DOI: 10.1016/j.cej.2023.147033.
16 S. H. Pyen, A. Mottafegh and D. P. Kim, *Chem. Eng. J.*, 2025, 163244, DOI: 10.1016/j.cej.2025.163244.
17 A. Mottafegh, J. U. Joo, G. S. Na, V. Sharma and D. P. Kim, *Chem. Eng. J.*, 2024, **500**, 157454, DOI: 10.1016/j.cej.2024.157454.

18 C. D. Chin, T. Laksanasopin, Y. K. Cheung, D. Steinmiller, V. Linder, H. Parsa, J. Wang, H. Moore, R. Rouse, G. Umviligihozo and E. Karita, *Nat. Med.*, 2011, **17**, 1015–1019, DOI: 10.1038/nm.2408.
19 M. Baumann, *Org. Biomol. Chem.*, 2018, **16**, 5946–5954, DOI: 10.1039/C8OB01437J.
20 I. Glasgow and N. Aubry, *Lab Chip*, 2003, **3**, 114–120, DOI: 10.1039/B302569A.
21 Z. Xian, P. Dai, W. Su, D. Xing, C. Sun and H. You, *J. Saudi Chem. Soc.*, 2023, **27**, 101755, DOI: 10.1016/j.jscs.2023.101755.
22 J. Luo, S. Song, H. Zhang, H. Zhang, J. Zhang and Y. Wan, *Eng. Life Sci.*, 2020, **20**, 441–450, DOI: 10.1002/elsc.202000018.
23 P. Jochems, Y. Satyawali, L. Diels and W. Dejonghe, *Green Chem.*, 2011, **13**, 1609–1623, DOI: 10.1039/C1GC15178A.
24 N. A. Alenazi, M. A. Hussein, K. A. Alamry and A. M. Asiri, *Des. Monomers Polym.*, 2017, **20**, 532–546, DOI: 10.1080/15685551.2017.1398208.
25 V. Sharma, J. U. Joo, A. Mottafegh and D. P. Kim, *Chem. Eng. J.*, 2025, 164284, DOI: 10.1016/j.cej.2025.164284.
26 Z. Mehrabi, Z. Harsij and A. Taheri-Kafrani, *J. Biotechnol.*, 2024, **394**, 1–10, DOI: 10.1016/j.jbiotec.2024.08.007.
27 J. Wang, C. Peng, X. Yang, M. Ni, X. Zhang, Z. Shi, H. Chen, S. Liu, L. Jin and C. Zhao, *Biomacromolecules*, 2023, **24**, 4170–4179, DOI: 10.1021/acs.biomac.3c00502.
28 J. H. Skerritt, M. Mayer and J. Francer, *Ther. Innov. Regul. Sci.*, 2025, **59**, 993–1003, DOI: 10.1007/s43441-025-00817-8.
29 P. Mantri, B. Juneja, S. Henderson, E. Koufos, Y. Moon, D. M. Dayeh, D. Di Grandi, Y. Fu, K. Muthusamy, P. M. Ihnat and N. Palackal, *J. Pharm. Biomed. Anal.*, 2024, **249**, 116352, DOI: 10.1016/j.jpba.2024.116352.
30 A. Dousis, K. Ravichandran, E. M. Hobert, M. J. Moore and A. E. Rabideau, *Nat. Biotechnol.*, 2023, **41**, 560–568, DOI: 10.1038/s41587-022-01525-6.
31 J. H. Kang, G. N. Ahn, H. Lee, S. J. Yim, S. Lahore, H. J. Lee, H. Kim, J. T. Kim and D. P. Kim, *ACS Cent. Sci.*, 2022, **8**, 43–50, DOI: 10.1021/acscentsci.1c00972.
32 M. Ottinger, I. Wenk, J. Carvalho Pereira, G. John and S. Junne, *Chem. Ing. Tech.*, 2022, **94**, 1883–1891, DOI: 10.1002/cite.202200105.